Available online at www.sciencedirect.com
SCIENCE DIRECT®
Fluid Phase Equilibria 216 (2004) 257–270
FLUID PHASE EQUILIBRIA
www.elsevier.com/locate/fluid

The next generation of hydrate prediction IV A comparison of available hydrate prediction programs

L. Ballard [a], E.D. Sloan Jr [b,*]

[a] *BP Amer0ica, Inc. 501 Westlake Park Blvd., Houston, TX 77079, USA*
[b] *Center for Hydrate Research, Colorado School of Mines1500 Illinois St., Golden, CO 80401-1887, USA*

Received 10 April 2003; accepted 14 November 2003

Abstract

The van der Waals and Platteeuw [Adv. Chem. Phys. 2 (1959) 1] hydrate equation of state, coupled with the classical thermodynamic equation for hydrates, has been used in the prediction of hydrate formation for over 40 years. The standard state used in these equations is a hypothetical empty hydrate lattice. In Part I of this series [Fluid Phase Equilib. 194/197 (2002) 371], we proposed an alternative derivation of these equations using a different standard state. The new hydrate equations were shown to be simpler to use. In Part II of this series [Fluid Phase Equilib. 211 (2003) 85], we proposed an aqueous phase model tailored specifically for the presence of mixed hydrate inhibitors such as salts and methanol in the aqueous phase. Part III [Fluid Phase Equilib. this volume] provided a prescription for the incorporation of the new hydrate and aqueous phase models into a multi-phase Gibbs energy minimization program (CSMGem), extending the work of Gupta and Bishnoi.

Part IV quantitatively compares the CSMGem program with four commercially available hydrate prediction programs: CSMHYD, DBRHydrate, Multiflash, and PVTsim. The work may be considered as a state-of-the-art accuracy overview of readily available hydrate prediction programs. Comparisons are given for two types of hydrate data: hydrate phase properties and hydrate formation temperatures and pressures. For the hydrate formation temperature and pressure comparisons, we show results for uninhibited and inhibited systems. Note that all data and predictions are at the incipient hydrate formation pressure (P) and temperature (T) due to lack of data for the interior of the phase diagrams. Such data await spectroscopic analysis for intrinsic variables and flash measurements for extrinsic properties, such as phase amounts, for comparison to flash calculation predictions.

Keywords: Hydrate; Gibbs energy minimization; Modeling; Spectroscopy

1. Introduction

This paper gives a quantitative discussion for the results of the hydrate parameter optimization. A comparison of predictions from CSMGem, the program developed in this work (Parts I-III of this series [2–4]), and four other commercial hydrate prediction programs, is given here for all recent hydrate data reported in literature. The four commercial programs compared in this work are:

CSMHYD	Colorado School of Mines (1998 Version)
DBRHydrate	DBRobinson Software Inc. (Version 5.0)
Multiflash	Infochem Computer Services Ltd. (Version 3.0)
PVTsim	Calsep A/S (Version 11)

Note that the hydrate model used in each of these programs stems from the original van der Waals and Platteeuw model [1]. The comparisons are broken into two categories: hydrate phase properties and hydrate formation temperatures and pressures. These comparisons show the accuracy that may be expected from readily available hydrate prediction programs. A brief overview connecting all four parts of this series is available [5].

2. Hydrate phase properties

What follows is a series of tables showing comparisons of experimental hydrate properties with predictions from several hydrate programs.

2.1. Fractional occupancy ratios

Table 1 shows the cage occupancy ratios (fraction of the large cages occupied by the guest, divided by the fraction

* Corresponding author. Tel.: +1-303-273-3723; fax: +1-303-273-3730.
E-mail address: esloan@mines.edu (E.D. Sloan Jr).

0378-3812/$ – see front matter © 2003 Elsevier B.V. All rights reserved.
doi:10.1016/j.fluid.2003.11.004

Table 1
Comparison of experimental and predicted cage occupancy ratios at 273.15 K and the equilibrium pressure

Hydrate	θ_L/θ_S (Data)	CSMGem	CSMHYD
Methane	1.156 [10] 1.053 [8] 1.092 [11] ($T = 233.15$ K)	1.146 1.116	1.118 1.064
Hydrogen sulfide	1.000 [9]	1.013	1.071
Carbon dioxide	8.333 [6]	1.908	1.347
Xenon	1.429 [8] 1.493 [9] 1.299 [7]	1.414	1.233

of the small cages occupied) for methane, hydrogen sulfide, xenon, and carbon dioxide hydrates at 273.15 K. Note that CSMGem and CSMHYD are the only hydrate programs that report the cage occupancies and are therefore the only program predictions to compare with data. Both programs give similar results for methane and hydrogen sulfide hydrates. However, for xenon hydrates, CSMHYD under predicts the data. For the carbon dioxide hydrate data, both programs under predict the reported value.The fractional occupancy ratio of methane hydrate has been extensively studied at temperatures other than 273.15 K. Sum et al. [12], Ripmeester and Ratcliffe [11], Jager [13], and Kini [14] have measured the fractional occupancy at several temperatures and pressures along the three-phase equilibrium line. Fig. 1 shows the predictions of CSMGem with their data. Note that the prediction by CSMGem does fairly well in reproducing the trend of the data by Subramanian and Jager. However, the data by Kini suggest a much larger occupancy ratio at low pressures and the data by Sum et al. suggest a completely different trend (increasing ratio with increasing pressure). It is unclear which sets of data, if any, are correct. It should be noted, however, that the data by Kini were taken using NMR spectroscopy whereas the other data sets were taken using Raman spectroscopy.

Assuming that the data by Jager (the largest number of points) are correct, CSMGem under predicts the pressure dependence shown in the data. That is, the data suggest that the ratio tends to unity more rapidly with pressure than the predictions. This may be an area in which the model may be further refined. Notice that the occupancy ratio has a different trend at pressures in which the hydrate forms below the ice point. The data of Kini confirm this trend.

2.2. Hydration number

The hydration number is the number of water molecules in the hydrate per guest molecule. Table 2 is a comparison of the experimental values for the hydration number for sI and sII hydrates at 273.15 K. All four hydrate programs predict the hydration number for methane, ethane, propane, and *i*-butane hydrates within reason. However, CSMGem, Multiflash, and CSMHYD all predict similar hydration numbers for hydrogen sulfide, but PVTsim predicts a much larger value. This is because PVTsim predicts hydrogen sulfide to form sII hydrates (which has fewer large cages to accommodate the hydrogen sulfide molecule) whereas the other hydrate programs predict hydrogen sulfide to form sI hydrates. The diffraction data [9] for the hydration number suggest that hydrogen sulfide forms sI hydrates. CSMGem predicts the xenon hydration number well, but CSMHYD under predicts the experimental value. Note that Multiflash and PVTsim do not contain xenon as a component so predictions could not be made. Also note that DBRHydrate does not report

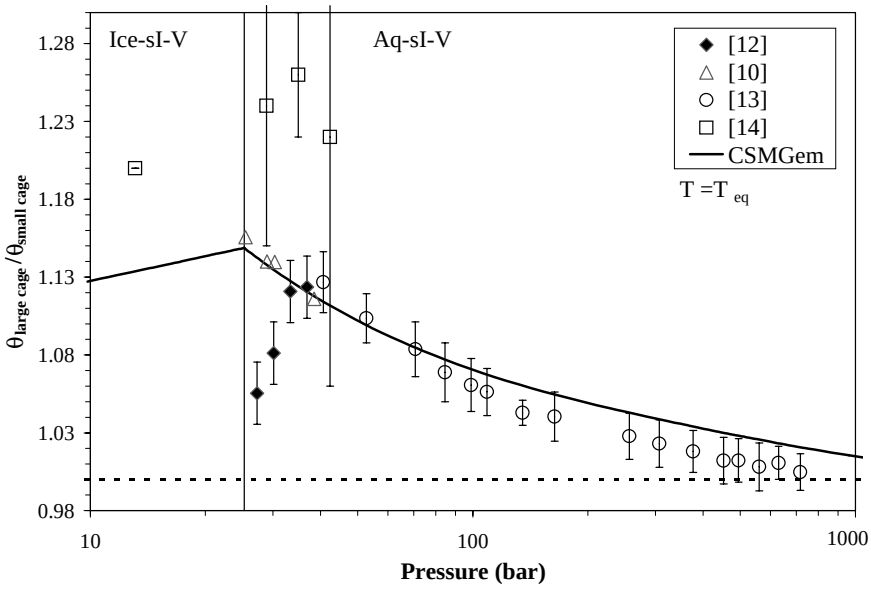

Fig. 1. Predictions of fractional occupancy ratio for sI methane hydrates [10,12–14].

Table 2
Comparison of experimental and predicted hydration numbers at 273.15 K

Hydrate	*n* (Data)	CSMGem	CSMHYD	Multiflash	PVTsim
Methane	5.77 [17] 6.00 [16,21] 6.30 [18] 7.4 [18] 7.00 [19] 7.18 [20]	6.300	6.073	6.100	6.046
Ethane	7.67 [16] 7.00 [19] 8.25 [20] 8.24 [21]	7.939	7.775	7.767	7.774
Propane	17.0 [9,16] 5.7 [22] 17.95 [20] 18.0 [23]	17.02	17.02	17.01	17.02
i-Butane	17.0 [16] 17.1 [15] 17.5 [24]	17.01	17.02	17.01	17.02
H_2S	6.12 [9]	6.241 (sI)	6.027 (sI)	6.106 (sI)	6.632 (sII)
Xenon	6.48 [9] 6.29 [15]	6.529	6.181	NA	NA

the overall composition of the hydrate so that comparisons could not be made.

The measured values of hydration number vary by as much as 28% for a given hydrate. We propose a possible explanation as to why there is such variance. In order to get hydration number, hydrates must be formed and then dissociated. Due to the highly metastable nature of forming hydrates (i.e. disordered system → ordered system), the pressure is typically increased above the equilibrium pressure (P_{eq}) until hydrates form, all at a given experimental temperature (T_{exp}). The pressure is then reduced, and hydrates are dissociated at the equilibrium temperature and pressure conditions (T_{exp}, P_{eq}). Fig. 2 gives an illustrative description of this process. Note that hydration numbers are typically reported at the experimental temperature and equilibrium temperature (T_{exp}, P_{eq}). However, it is not necessarily true that the hydration numbers were formed at those conditions.

Thermodynamics dictates that, for a binary system of a hydrate former and water, hydrates must form at the three-phase equilibrium line Aq–H–V. Since the pressure of the system equilibrates much faster than the temperature, it follows that, at a given experimental pressure (P_{exp} in

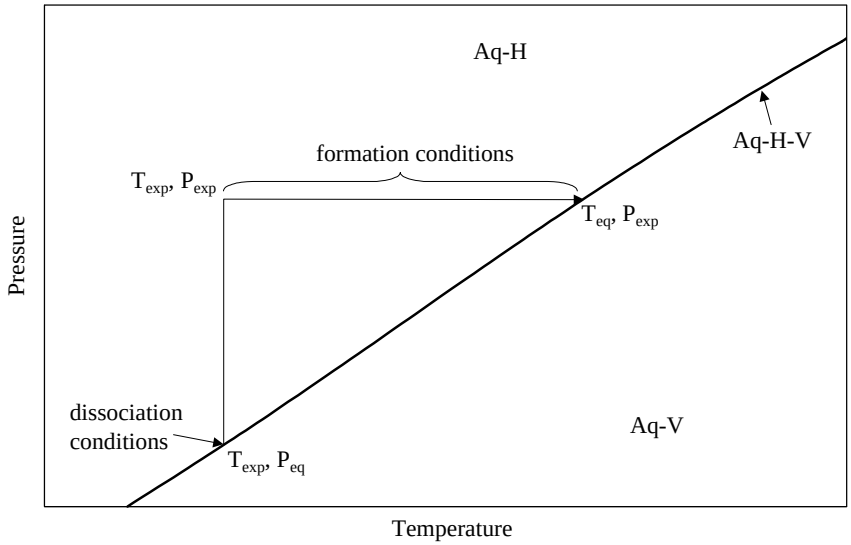

Fig. 2. Hydrate formation process for single hydrate.

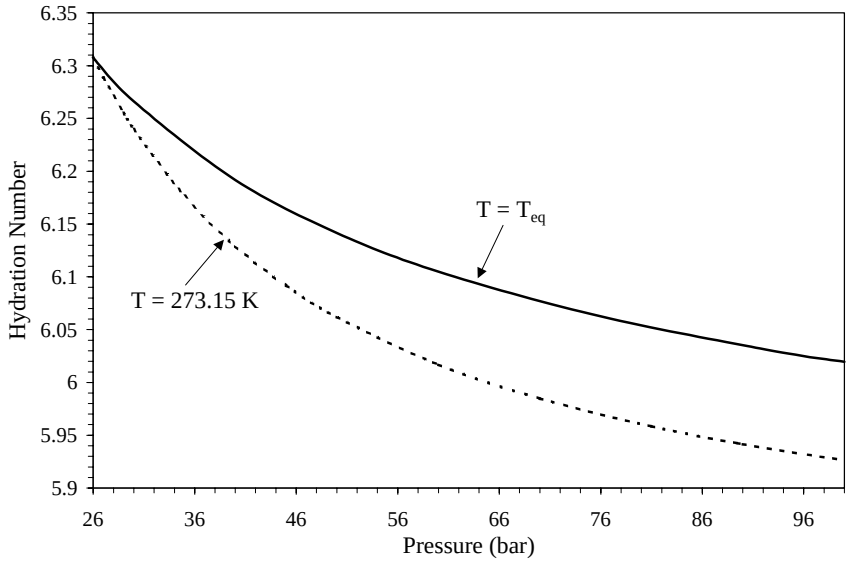

Fig. 3. Methane hydrate hydration numbers at pressures higher than equilibrium (26 bar) at $T = 273.15$ K.

Fig. 2), the hydrate must form at the equilibrium temperature (T_{eq}, P_{exp}) [25]. Due to heat transfer effects, however, the hydrate may form at the P_{exp} and some temperature between T_{eq} and T_{exp}. Therefore, the hydrate formed is not at T_{exp} and P_{eq}, but rather at P_{exp} and $T_{exp} < T < T_{eq}$. Assuming that solid phase diffusion is negligible, the hydration number obtained by dissociating the hydrate will not be the true hydration number at T_{exp} and P_{eq}.

To test the hydration numbers reported in Table 2, Fig. 3 was plotted for the hydration numbers of methane hydrates at several pressures. Two curves are given: the solid line is the predicted hydration number at pressures and temperatures along the three-phase equilibrium line and the dashed line is the predicted hydration number at 273.15 K and pressures higher than P_{eq}. From the above argument, the true hydration number should be somewhere between these lines. If this hypothesis is true, the reported experimental hydration numbers are lower than the three-phase equilibrium values. This would suggest why Table 2 shows such a large deviation within the groups of experimental values of hydration number at 273.15 K. That is, each experimenter may have formed the hydrates at different pressures. Such an explanation may also apply to the reason CSMGem tends to slightly over predict the experimental values.

2.3. Structural transitions of methane + ethane hydrates

Another crucial piece of hydrate data is the structural transition composition. Hydrate structural transition data give the composition, temperature, and pressure at which two hydrates are present at the formation conditions. Subramanian et al. [26,27] showed two structural transitions between sI and sII for methane + ethane hydrates. Table 3 is a comparison of the experimental values for the structural transition compositions of the methane + ethane + water system at 274.15 K. Note that Multiflash and PVTsim both under predict the lower composition whereas CSMGem predicts the value within experimental error. The upper composition is predicted well by all three programs. This is important to note since it could have applications for natural hydrates in the permafrost and deep-sea sediments. It also should be noted that CSMHYD predicts the methane + ethane + water system will form sI hydrates along the entire composition extreme. DBRHydrate does not report hydrate structure so a comparison could not be made.

2.4. Hydrate formation temperatures and pressures for uninhibited systems

The most common type of hydrate data taken is the formation temperatures and pressures. This type of data is most important to natural gas applications. We have compiled all experimental data of this type and compared it with predictions from CSMGem, CSMHYD, DBRHydrate, Multiflash, and PVTsim. It should be noted that DBRHydrate has a prediction limit to pressures below 680 bar and so comparisons could not be made for higher pressure data. A total of 1685 hydrate formation data points were used in the comparison.

A series of figures follow, giving the average errors in temperature and pressure for several types of hydrates based on the following categories: (1) single hydrates, (2) binary hydrates, (3) ternary hydrates, (4) multi-component hydrates

Table 3
Comparison of experimental and predicted structural transition composition at 274.15 K for the methane + ethane + water system

Data	CSMGem	Multiflash	PVTsim
0.736 ± 0.014 [26]	0.722	0.600	0.668
0.993 ± 0.006 [27]	0.994	0.994	0.992

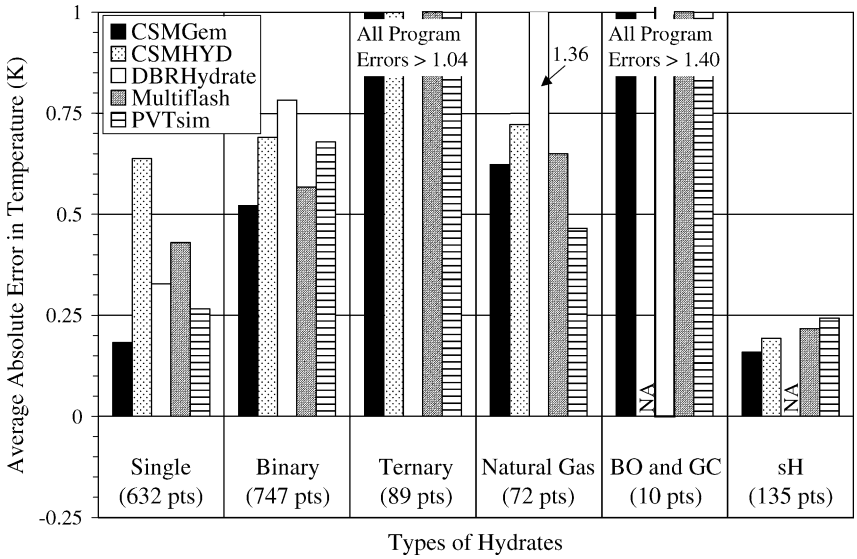

Fig. 4. Hydrate formation T error (absolute) for all types of hydrates.

(natural gas hydrates), (5) hydrates in black oils (BO) and gas condensates (GS), and (6) sH hydrates. The results are given as the average error either in temperature or pressure. The average absolute error in temperature and pressure are calculated as:

$$T_{\text{Error}} = \frac{\sum_{\#\text{datapoints}} |T_{\text{predicted}} - T_{\text{experimental}}|}{\#\text{datapoints}} \quad (1)$$

$$P_{\text{Error}} = \frac{\sum_{\#\text{datapoints}} |P_{\text{predicted}} - P_{\text{experimental}}| / P_{\text{experimental}}}{\#\text{datapoints}} 100\% \quad (2)$$

and are given in Kelvin and bar, respectively. The next section will give the comparisons, discussing major differences in the models. A more complete listing of the results can be found in Ballard [28].

Figs. 4 and 5 provide average absolute temperature and pressure errors (Eqs. (1) and (2) for the different data groupings. The number of data points used in the comparisons is given at the bottom of each column. Fig. 6 is the average absolute temperature and pressure errors over all the data points. The average absolute errors in temperature for CSMGem, CSMHYD, DBRHydrate, Multiflash, and PVTsim are 0.40, 0.66, 0.64, 0.54, and 0.54 K, respectively. For pressure, the errors are 6, 9, 10, 9, and 11%, respectively. The average absolute temperature and pressure error for CSMGem is more than 25 and 31% lower than the next smallest errors, respectively.

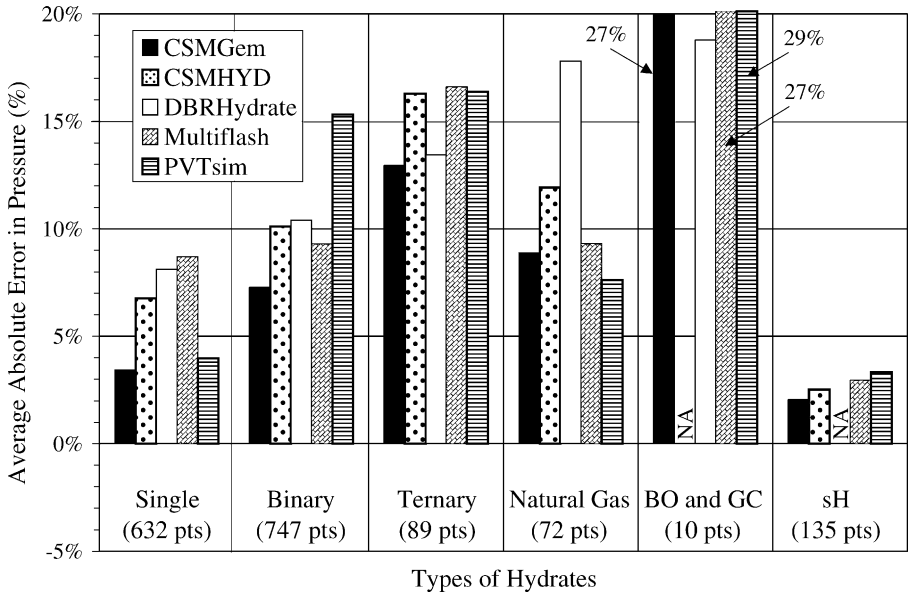

Fig. 5. Hydrate formation P error (absolute) for all types of hydrates.

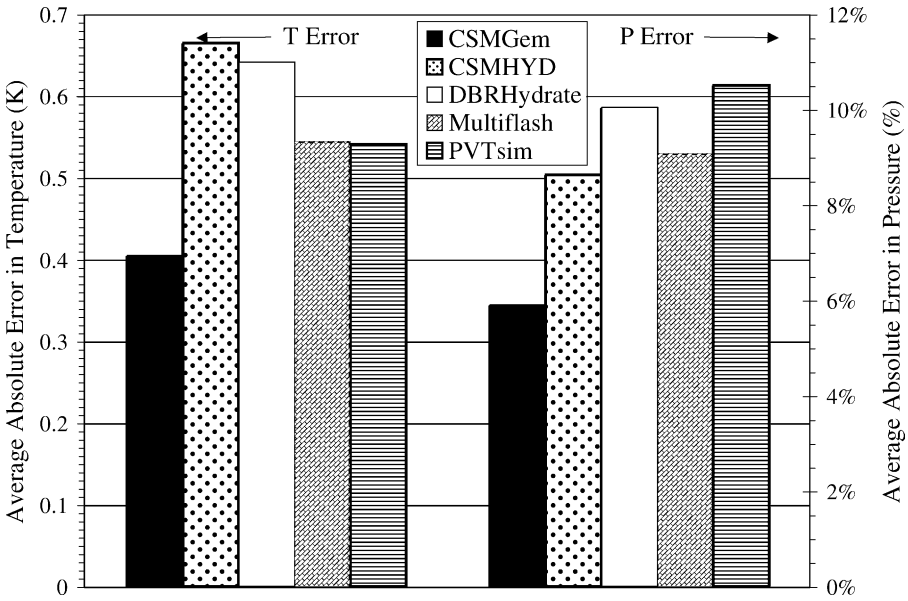

Fig. 6. Hydrate formation T and P errors (absolute) for all hydrates (1685 pts).

All programs give large error for the ternary, black oil, and gas condensate hydrates. This is most likely due to error in the data for the ternary hydrates. However, for the BO and GC hydrates, the error may be in the characterization of the heavy hydrocarbon components.

3. Analysis of uninhibited systems

What follows are analyses of the more interesting hydrate systems. In particular, we will discuss interesting predictions for single, binary, multi-component, black oil and gas condensate, and sH hydrates.

3.1. Single hydrates

The most notable differences between CSMGem the other hydrate programs are in the methane and carbon dioxide single hydrates. As shown in Figs. 7 and 8, the methane + water and carbon dioxide + water pressure versus temperature phase diagrams, the experimental data suggest a maximum temperature at which hydrates form (∼321 and ∼294 K, respectively). This phenomenon is called retrograde behavior, in which hydrates will dissociate upon pressurization at a given temperature. For ease of interpretation, predictions from DBRHydrate, PVTsim, and CSMHYD are not given, however predictions from these programs are

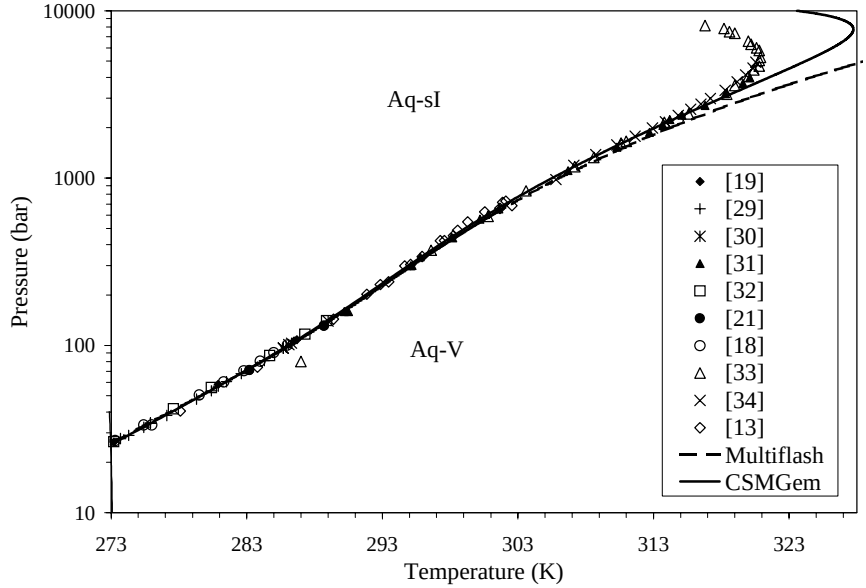

Fig. 7. P vs. T phase diagram for methane + water system [13,18,19,21,29,30–34].

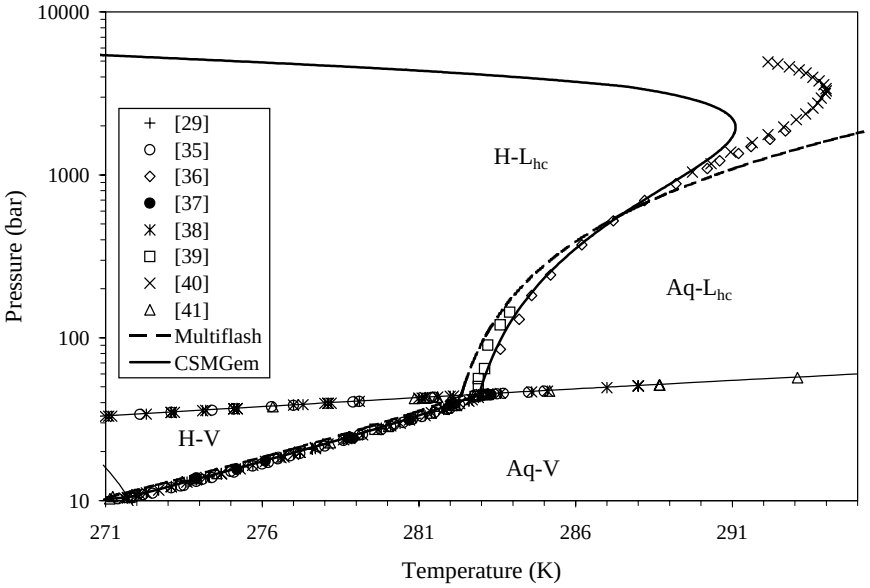

Fig. 8. *P* vs. *T* phase diagram for carbon dioxide + water system [29,35–41].

similar to those of Multiflash. Note that the CSMGem predictions give the same trend as the data whereas the Multiflash predictions do not. The differences in the trends of the predictions between CSMGem and the other programs is due to the treatment of the hydrate volume as a function of temperature and pressure. As the pressure is increased, the hydrate volume compresses, thus reducing the size of the hydrate cages. At some temperature and pressure (as determined by the data), the small cages may become so small that the guest molecule can no longer fit into them to stabilize the hydrate. Beyond this temperature hydrates cannot form.

Another interesting difference between the models is in the nitrogen + water system. CSMGem predicts a structural transition between sI and sII hydrates at approximately 280.2 K and 334.8 bar, as shown in Fig. 9. CSMHYD predicts sII hydrate for the entire three-phase equilibrium line for nitrogen hydrates, whereas Multiflash and PVTsim predict sI hydrates. The structure of nitrogen hydrates has been a question that has never been acceptably answered. Kuhs et al. [45] have done several neutron diffraction measurements on nitrogen hydrates at 273.15 K and many pressures up to 2500 bar. However, they found both sI and sII hydrates of nitrogen present at these conditions.

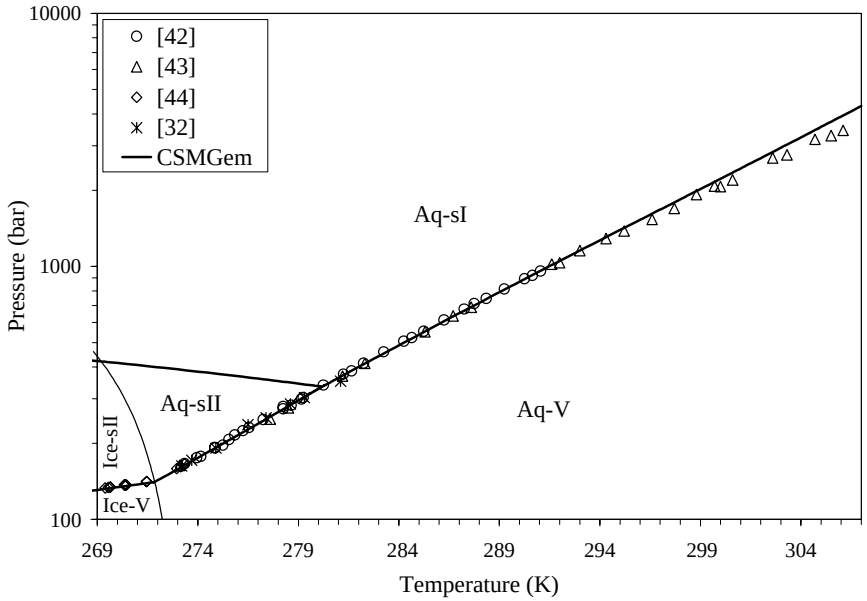

Fig. 9. *P* vs. *T* phase diagram for nitrogen + water system [32,42–44].

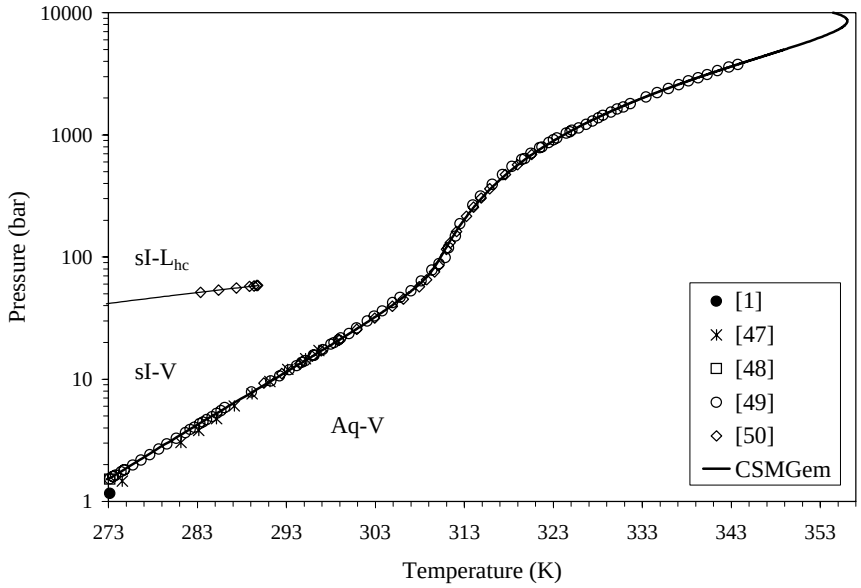

Fig. 10. *P* vs. *T* phase diagram for xenon + water system [1,47–50].

The predictions from CSMGem support their observations that both structures could possibly form, with one being metastable. Since we know that nitrogen doubly occupies the large cages of sI and sII hydrates, which CSMGem does not account for, a future modification may be to account for double occupancy in order to predict the data at higher pressures.

Another noteworthy prediction is that of xenon + water hydrates. The work by Dyadin et al. [46] suggests that xenon hydrates exhibit retrograde behavior at high pressure. Experimental three-phase equilibrium data for xenon hydrates do not go beyond 3800 bar in pressure. However, as shown in Fig. 10, CSMGem predicts that xenon hydrates do have a maximum temperature of formation at 356 K (8578 bar). As can be seen in Fig. 10, the hydrate formation data are modeled very well at all pressures and temperatures for xenon hydrates. Since xenon is a spherical molecule, the hydrate model should be able to model xenon hydrates especially well. This is because of the inherent assumption of a spherical guest molecule in the Kihara spherical core potential model. The favorable predictions of the xenon + water system at all conditions gives validity to the CSMGem hydrate model. However, it may give reason for further refinement to the treatment of non-spherical guest molecules in the potential model.

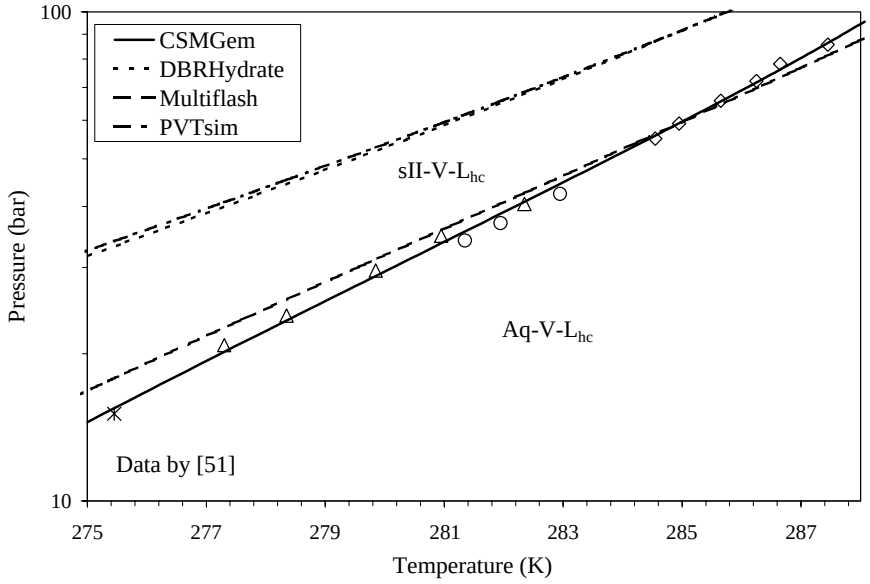

Fig. 11. *P* vs. *T* phase diagram for methane + benzene + water system [51].

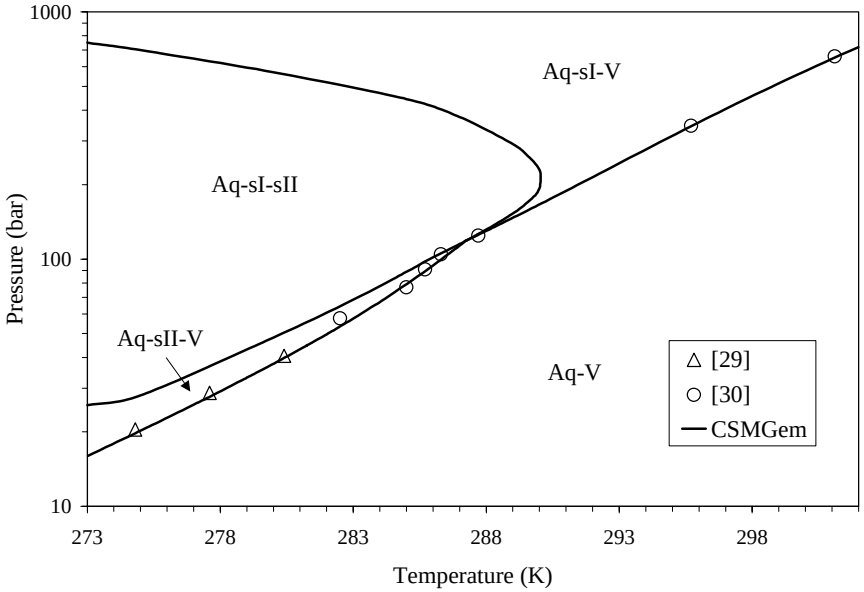

Fig. 12. *P* vs. *T* phase diagram for methane(0.974) + *n*-butane(0.026) + water(excess) system [29,30].

3.2. Binary hydrates

Another notable difference between CSMGem and all other hydrate programs is found in the methane + benzene hydrate. Benzene is a very large molecule and therefore cannot form sII hydrates without the presence of a "help" molecule such as methane. Fig. 11 shows the pressure versus temperature phase diagram for this system. Note that the overall composition of the system is not needed since the four-phase equilibrium line (Aq–sII–V–L_{hc}) is univariant by Gibbs phase rule. CSMGem straddles the experimental data and predicts the correct trend (or slope) while Multiflash differs slightly. We believe this is due to treatment of large guest molecules in the hydrate lattice (via the volume model and hydrate cage description). Note that DBRHydrate and PVTsim predict sI hydrates to be more stable (with only methane being incorporated into the hydrate), and therefore, these programs have large errors in the predicted formation temperature.

An interesting prediction to be noted is that of the methane + *n*-butane hydrates. Predictions show that there are several structural transitions: sII hydrates at low pressure and sI hydrates at higher pressure. Fig. 12 is a phase equilibria plot for this system. The hydrate formation predictions

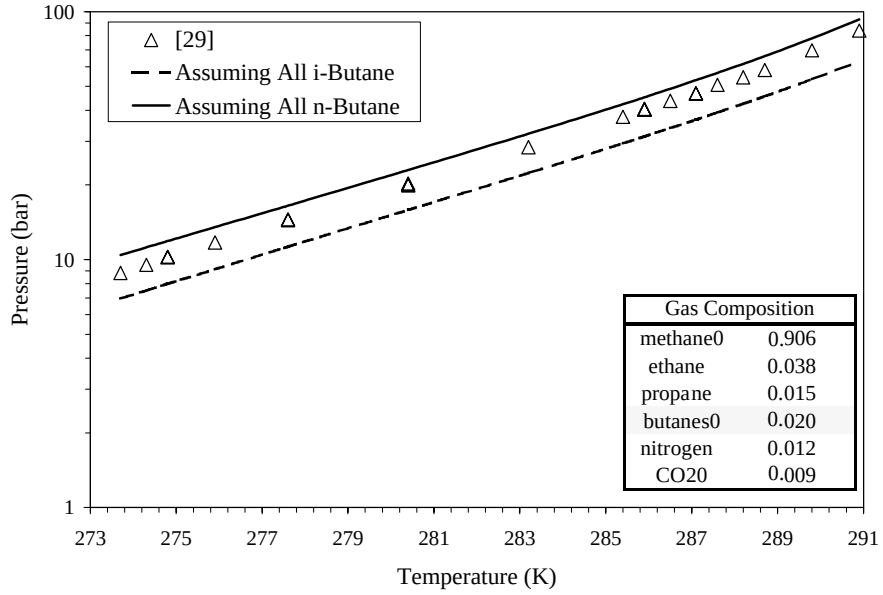

Fig. 13. *P* vs. *T* phase diagram for a natural gas hydrate showing the sensitivity of the predictions to the butane content [29].

from CSMGem match the data by Deaton and Frost [29] and McLeod and Campbell [30] well. Note that past workers have discounted the high pressure data of McLeod and Campbell on the basis of non-linearity on a semi-logarithmic plot. However, the high pressure (>120 bar) data by McLeod and Campbell are predicted to be sI hydrates. This is interesting because hydrates of methane and n-butane are usually considered to be sII. Also note the large region in which sI and sII hydrates are predicted to coexist with an aqueous phase. It is diagrams such as Fig. 12 that show the benefits of using the Gibbs energy minimization technique to predict at pressures above the hydrate formation conditions.

Table 4
Complete listing of natural gas hydrate formation data

Researcher	Number of gases	Data points	Year
Wilcox et al. [52]	3	36	1941
Deaton and Frost [29]	11	90	1946
Kobayashi et al. [53]	2	10	1951
McLeod and Campbell [30]	1	7	1961
Lapin and Cinnamon [54]	3	3	1969
Adisasmito and Sloan [55]	5	20	1992
Bishnoi and Dholabhai [56]	1	3	1999
Jager [13]	1	17	2001
	27	186	

3.3. Multi-component hydrates

Hydrate formation data for natural gases are probably the most important type of data from an industrial perspective. It is also important for the purpose of validating the hydrate model. However, very few data have been taken for hydrates of natural gases. Therefore, it is difficult to determine the accuracy of hydrate programs for “real” systems.

Deaton and Frost [29] determined hydrate formation points for several natural gas hydrates, however, due to the crude analysis available at that early date they did not report the butane analysis for each gas mixture (i.e. separate compositions of *i*-butane and *n*-butane). Because of this, we performed a sensitivity analysis to determine the affect of the composition of i- and n-butane on hydrate stability. Fig. 13 is a pressure versus temperature phase diagram for one of the typical Deaton and Frost natural gas hydrates. Note that, in the report of the gas composition, the individual butane amounts were not specified. Two cases were studied: (1) assuming the entire butane amount was *i*-butane (dashed line) and (2) assuming the entire butane amount was *n*-butane (solid line). As seen in Fig. 13, the hydrate formation temperatures and pressures are very sensitive to the relative amount of butanes in the natural gas mixture. In fact, the difference in predicted hydrate formation pressure for both cases ranged from 15 to 50% (1.0–4.0 K in predicted temperature) depending on the overall gas composition and relative amount of butanes. Therefore, the Deaton and Frost natural gas data could not be used to compare the different hydrate program predictions.

A complete listing of all researchers reporting hydrate formation points for natural gases is given in Table 4. Unfortunately, the number of data points measured by Deaton and Frost comprise almost 50% of the total amount of data for natural gas hydrates in the past 60 years.

It should be noted that the data by McLeod and Campbell [30] and Jager [13] are at fairly high pressure. This type of data is helpful in that the trend of the data at high pressure can be compared to the prediction programs. An interesting anomaly associated with the processed natural gas hydrate data by Jager [13] is that, at high pressure, the equilibrium

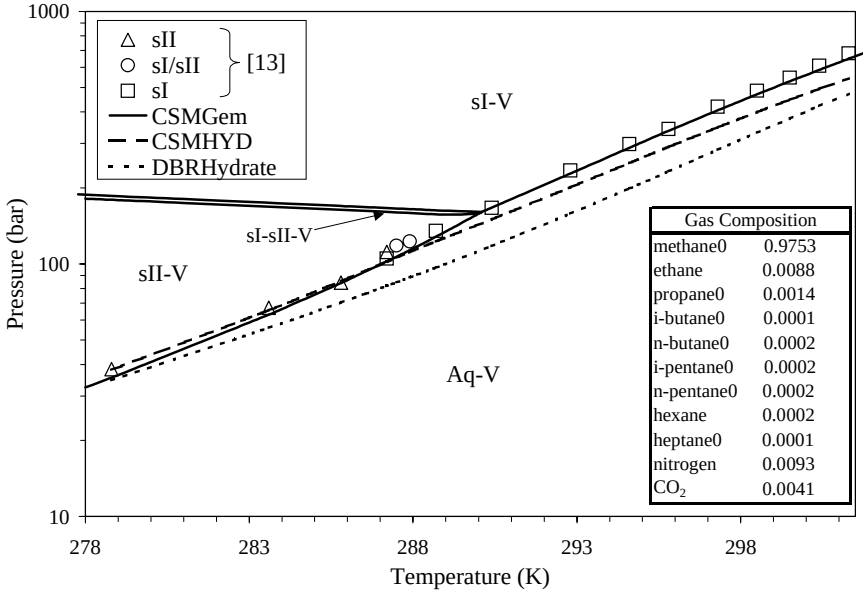

Fig. 14. *P* vs. *T* phase diagram for processed natural gas [13].

hydrate changes from sII to sI. This phenomenon has been observed in many systems such as methane + ethane + water and methane + *i*-butane + water. However, it has not been observed for a natural gas. Fig. 14 is the pressure versus temperature phase diagram for the processed natural gas. While all programs predict the structural transition to occur, the high pressure behavior of CSMHYD and DBRHydrate, shown in Fig. 14 as the long- and short-dashed lines, respectively, are inconsistent with the experimental data. Again, this is indicative of the correct high pressure treatment of the hydrate phase by CSMGem. Predictions by PVTsim and Multiflash are similar to those of CSMGem.

One of the major conclusions made after reviewing the available natural gas hydrate data in the literature is that there are not enough data to make a complete comparison between the different hydrate programs. The majority of the available data are not relevant for natural gas pipeline flow assurance. The Deaton and Frost data cannot be used because of the lack of butane analysis, the Adisasmito and Sloan data cannot be used because of the high carbon dioxide content, and the Jager data cannot be used because they are for a processed natural gas. This leaves only 59 (out of 189) data points for 10 (out of 27) natural gases to make the comparisons. Because of this, more data for relevant natural gases are needed.

Table 5
Composition of gas condensate #1a–a used in calculations

Component	Mole fraction
N2	0.00193
CO2	0.00098
C1	0.96373
C2	0.00862
C3	0.00531
i-C4	0.00109
n-C4	0.0026
i-C5	0.00109
n-C5	0.00138
C6	0.00194
m-c-c5	0.00041
Benzene	0.00003
c-c6	0.00025
C7	0.00252
C8	0.00192
C9	0.00147
C10	0.00112
C11	0.00086
C12	0.00065
C13	0.0005
C14	0.00038
C15	0.00029
C16–17	0.00039
C18–20	0.0003
C21–53	0.00024

3.4. Black oil and gas condensate hydrates

The most stringent test for a hydrate program is to compare predictions with experimental hydrate data in black oils and gas condensates. These types of predictions are a more stringent test on the hydrocarbon equation of state than the hydrate model because of the complex hydrocarbon mixtures involved. An interesting note is that the predictions suggest a structural transition from sII to sI for the gas condensate hydrates studied. Table 5 gives the composition of the gas condensate. Fig. 15 is the pressure versus temperature phase diagram for the gas condensate system. The structural transition pressures are predicted to occur at 340 bar (CSMGem), 120 bar (DBRHydrate), 290 bar (PVTsim), and 260 bar (Multiflash) for each prediction program. Note that predictions from DBRHydrate and CSMGem are essentially

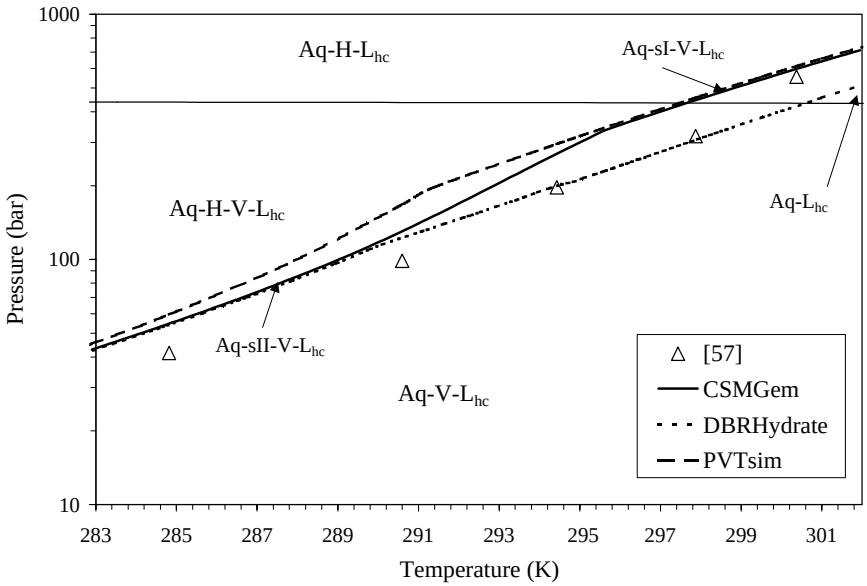

Fig. 15. *P* vs. *T* phase diagram for gas condensate [57].

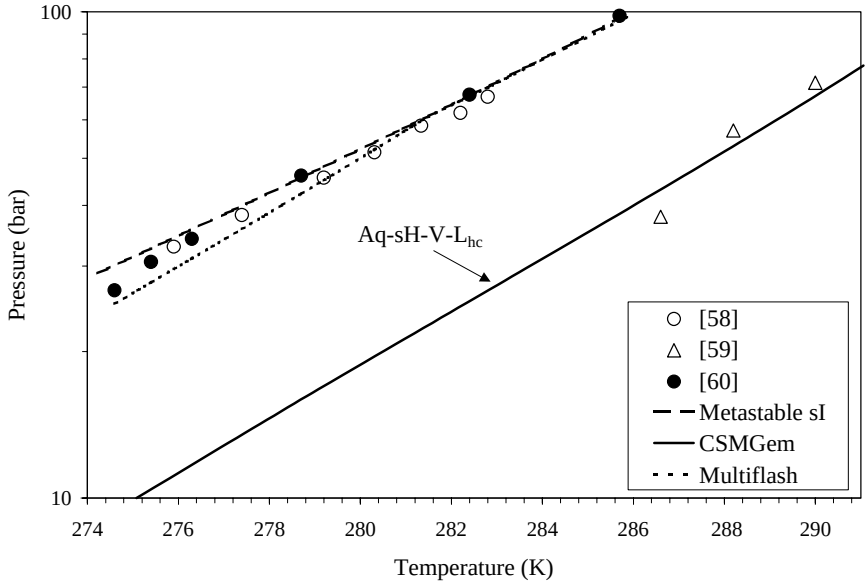

Fig. 16. *P* vs. *T* phase diagram for methane + 2,2-dimethylpentane hydrate [58–60].

identical in the sII region (low *P*) while predictions from PVTsim and CSMGem are essentially identical in the sI region (high *P*). Predictions from Multiflash are not shown but are similar to those of CSMGem. Note that DBRHydrate predictions straddle the data, which leads to a small overall average error.

3.5. sH Hydrates

A less common hydrate in natural gas systems is sH hydrate. sH hydrate forms when a large molecule such as i-pentane is in the presence of a "help" molecule such as methane. All applicable programs do a relatively good job in predicting sH hydrate formation. Note that DBRHydrate does not have the capability to predict sH hydrates and therefore cannot be compared with the other programs.

The selection of data for parameter optimization was done with care. Fig. 16 is the pressure versus temperature phase diagram for the hydrate formation conditions reported in the literature for the methane + 2,2-dimethylpentane hydrate. The data by Mehta and Sloan [58] and Østergaard et al. [60] are quite different than those of Thomas and Behar [59]. Because of this, we predicted the metastable sI hydrate prediction (long-dashed line) for this system and concluded that the data by Thomas and Behar represents the sH hydrate correctly. Therefore, these are the data we

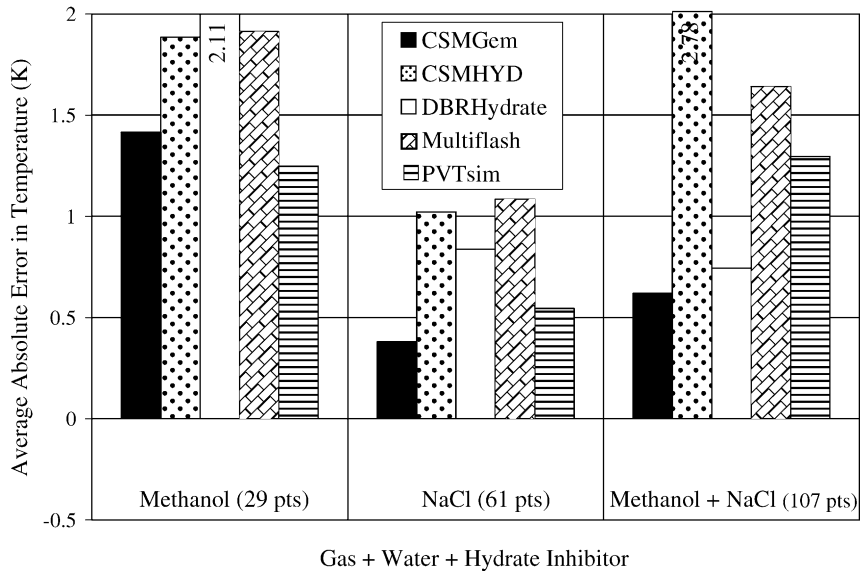

Fig. 17. Hydrate formation *T* error (absolute) for all inhibited hydrates.

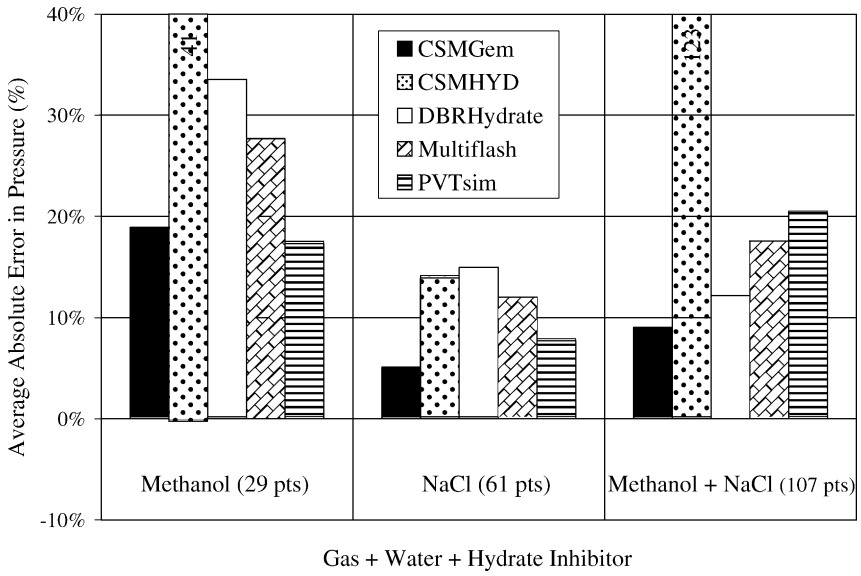

Fig. 18. Hydrate formation P error (absolute) for all inhibited hydrates.

used in the optimization. In systems such as this, it would be ideal if spectroscopic measurement [26,27] of the hydrate phase were made to define the correct sH hydrate equilibrium conditions.

4. Hydrate formation temperatures and pressures for inhibited systems

The next step was to compare the hydrate prediction programs with hydrate formation temperatures and pressures for inhibited systems. In particular, we show predictions for systems containing methanol, sodium chloride salt (NaCl), and mixtures of the two.

Figs. 17 and 18 are the average absolute temperature and pressure errors (Eqs. (1) and (2) for the three different types of inhibited systems. The number of data points used in the comparisons is given at the bottom of each column. It should be noted that each hydrate prediction program consistently under- or over-predicts inhibited hydrate data. However, for nearly all inhibited systems, CSMGem predicts the data with less error than the other programs. A complete analysis of modeling inhibited hydrate systems can be found in Jager [13].

5. Conclusions

In conclusion, CSMGem compares favorably to other hydrate programs. It is quite an improvement on the previous hydrate prediction program from this laboratory (CSMHYD). It also is an improvement over the DBRHydrate program, especially at high pressure.

After reviewing the available natural gas hydrate data in the literature, we conclude that there are not enough data to make a complete comparison between the different hydrate programs. There are only 59 data points for 10 relevant natural gases (i.e. natural gases of industrial interest). Likewise, there are too few black oil and gas condensate hydrate data available.

The hydrate formation temperatures and pressures for uninhibited systems are predicted quite well by CSMGem, giving credibility to the proposed hydrate model (discussed in Part I of this series). The favorable predictions for inhibited systems give credibility to the aqueous phase model (discussed in Part II of this series). CSMGem not only predicts the hydrate formation temperature and pressures well, but it also predicts hydrate properties and the interior of hydrate phase diagrams. The lower structural transition composition reported by Subramanian et al. is matched well, while Multiflash and PVTsim under predict the composition by 10 and 6 mol%, respectively, and CSMHYD and DBRHydrate do not predict a transition at all.

List of Symbols

P	presure
T	temperature

Greek Letter

θ	hydrate cage fractional occupancy, stability variable

Subscripts

eq	equilibrium conditions
exp	experimental conditions

References

[1] J.H. van der Waals, J.C. Platteeuw, Adv. Chem. Phys. 2 (1959) 1–57.
[2] A.L. Ballard, E.D. Sloan Jr, Fluid Phase Equilib. 194 (2002) 371–383.

[3] M.D. Jager, A.L. Ballard, E.D. Sloan Jr, Fluid Phase Equilib. 211 (2003) 85–107.
[4] A.L. Ballard, E.D. Sloan, Jr., Fluid Phase Equilib., this volume.
[5] A.L. Ballard, E.D. Sloan, Jr., in: Proceedings of the Fourth International Conference on Gas Hydrates, Yokohama, Japan, May 19-23, 2002, 307–314, available on CD through icgh@mori.mech.keio.ac.jp.
[6] D.W. Davidson, in: L. Cox (Ed.), Natural Gas Hydrates: Properties, Occurrence, and Recovery, Butterworths, Boston, 1983.
[7] J.A. Ripmeester, D.W. Davidson, J. Mol. Struct. 75 (1981) 67–72.
[8] J.S. Tse, D.W. Davidson, in: Proceedings of the Fourth Canadian Permafrost Conference, March 2-6, 1981, Calgary, Alberta, Canada, pp. 329–334.
[9] G.H. Cady, J. Phys. Chem. 87 (1983) 4437–4441.
[10] S. Subramanian, Ph.D. thesis, Colorado School of Mines, 2000.
[11] J.A. Ripmeester, C.I. Ratcliffe, J. Phys. Chem. 92 (1988) 337–339.
[12] A.K. Sum, R.C. Burruss, E.D. Sloan Jr, J. Phys. Chem. B 101 (1997) 7371–7377.
[13] M.D. Jager, Ph.D. thesis, Colorado School of Mines, 2001.
[14] R. Kini, Ph.D. thesis, Colorado School of Mines, 2002.
[15] T. Uchida, I. Hayano, Rep. Govt. Chem. Ind. Res. Inst. Tokyo 59 (1964) 382–387.
[16] Y.P. Handa, AIChE Meeting, November 2–7, 1986, Miami Beach, FL.
[17] D.N. Glew, J. Phys. Chem. 66 (1962) 605.
[18] J.L. de Roo, C.J. Peters, R.N. Lichtenthaler, G.A.M. Diepen, AIChE J. 29 (1983) 651–657.
[19] O.L. Roberts, E.R. Brownscombe, L.S. Howe, H. Ramser, Petrol Eng. 12 (1941) 56.
[20] E.M. Frost Jr, W.M. Deaton, Oil Gas J. 45 (1946) 170–178.
[21] T.J. Galloway, W. Ruska, P.S. Chappelear, R. Kobayashi, Ind. Eng. Chem. Fund. 9 (1970) 237–243.
[22] B. Miller, E.R. Strong Jr, Am. Gas Assoc. Monthly 28 (1946) 63.
[23] W.G. Knox, M. Hess, G.E. Jones, H.B. Smith, Chem. Eng. Prog. 57 (1961) 66.
[24] O.S. Rouher, A.J. Barduhn, Desalination 6 (1969) 57.
[25] E.M. Freer, M.Sc. thesis, Colorado School of Mines, 2000.
[26] S. Subramanian, R. Kini, S.F. Dec, E.D. Sloan Jr, Chem. Eng. Sci. 55 (2000) 1981–1999.
[27] S. Subramanian, A.L. Ballard, R. Kini, S.F. Dec, E.D. Sloan Jr, Chem. Eng. Sci. 55 (2000) 5763–5771.
[28] A.L. Ballard, Ph.D. thesis, Colorado School of Mines, 2002.
[29] W.M. Deaton, E.M. Frost, US Bureau Mines Monogr. 8 (1946) 101.
[30] H.O. McLeod, J.M. Campbell, J. Pet. Tech. 222 (1961) 590–597.
[31] D.R. Marshall, S. Saito, R. Kobayashi, AIChE J. 10 (1964) 202–205.
[32] J. Jhaveri, D.B. Robinson, Can. J. Chem. Eng. 43 (1965) 75–78.
[33] Y.A. Dyadin, E.Y. Aladko, in: Proceedings of the Second International Conference on Gas Hydrates, Toulouse, France, June 2–6 1996, pp. 67–70.
[34] S. Nakano, M. Moritoki, K. Ohgaki, J. Chem. Eng. Data 44 (1999) 254–257.
[35] S.D. Larson, Ph.D. thesis, University of Illinois, 1955.
[36] S. Takenouchi, G.C. Kennedy, J. Geol. 73 (1965) 383–390.
[37] D.B. Robinson, B.R. Mehta, J. Can. Pet. Tech. 10 (1971) 33.
[38] J.G. Vlahakis, H.-S. Chen, M.S. Suwandi, A.J. Barduhn, Syracuse University, Research and Development Report 830, prepared for US Department of the Interior, November 1972.
[39] H.-J. Ng, D.B. Robinson, Fluid Phase Equilib. 21 (1985) 145.
[40] S. Nakano, M. Moritoki, K. Ohgaki, J. Chem. Eng. Data 43 (1998) 807–810.
[41] M. Wendland, H. Hasse, G. Maurer, J. Chem. Eng. Data 44 (1999) 901–906.
[42] A. van Cleeff, G.A.M. Diepen, Rec. Trav. Chim. 79 (1960) 582–586.
[43] S. Saito, D.R. Marshall, R. Kobayashi, AIChE J. 10 (1964) 734–740.
[44] A. van Cleeff, G.A.M. Diepen, Rec. Trav. Chim. 84 (1965) 1085–1093.
[45] W.F. Kuhs, B. Chazallion, P. Radaelli, F. Pauer, J. Kipfstuhl, in: Proceedings of Second International Conference Natural Gas Hydrates, June 2–6, 1996, Toulouse, France, pp. 9–16.
[46] Y.A. Dyadin, E.G. Larionov, T.V. Mikina, L.I. Starostina, Mendeleev Commun. 6 (2) (1996) 44–45.
[47] R. de Forcrand, Comput. Rend. 181 (1925) 15–17.
[48] R.M. Barrer, A.V.J. Edge, Proc. Roy. Soc. (Lond.) A300 (08/22) (1967) 1–24.
[49] L. Aaldijk, Ph.D. thesis, Tech. Univ. Delft, 1971.
[50] K. Ohgaki, T. Sugahara, M. Suzuki, H. Jindai, Fluid Phase Equilib. 175 (2000) 1–6.
[51] A. Danesh, B. Tohidi, R.W. Burgass, A.C. Todd, Trans. IChemE 71A (1993) 457.
[52] W.I. Wilcox, D.B. Carson, D.L. Katz, Ind. Eng. Chem. 33 (1941) 662.
[53] R. Kobayashi, H.J. Withrow, G.B. Williams, D.L. Katz, Proc. Conf. NGAA 30 (1951) 27–31.
[54] A. Lapin S.J. Cinnamon, Proc. Liquid Natural Gas: its Production, Handling, and Use, London, 1969, p. 198.
[55] S. Adisasmito, E.D. Sloan Jr, J. Chem. Eng. Data 37 (1992) 343–348.
[56] P.R. Bishnoi, P.D. Dholabhai, Fluid Phase Equilib. 158-160 (1999) 821–827.
[57] P.K. Notz, Personal and e-mail communication, May 2001.
[58] A.P. Mehta, E.D. Sloan Jr, J. Chem. Eng. Data 39 (1994) 887–890.
[59] M. Thomas, E. Behar, in: Proceedings of the 73rd GPA Convocation, New Orleans, LA, March 7–9, 1994, p. 100.
[60] K.K. Østergaard, B. Tohidi, A. Danesh, R.W. Burgass, A.C. Todd, Fluid Phase Equilib. 169 (2000) 101–115.